COMPUTER SIMULATION OF PLATELET ACTIVATION IN A PULSATILE VENTRICULAR ASSIST DEVICE, THROUGH FINITE ELEMENTS AND A SIMPLIFIED GEOMETRY

E.R. FRÍES, M.E. BERLI, S. UBAL, D.M. CAMPANA   and   J. DI PAOLO

Grupo Biomecánica Computacional, Facultad de Ingeniería, Univ. Nac. de Entre Ríos
Ruta 11, km 10, 3100 Oro Verde, Entre Ríos, Argentina
efries@bioingenieria.edu.ar

Abstract— **Ventricular assist devices are a technological solution for patients who suffer from cardiac insufficiency and await a transplant. In this work, a new design of an implantable pulsatile blood pump is analyzed in terms of blood damage, by means of finite elements on a simplified geometry. It is a double effect volumetric pump, which has a non-contact driven piston and four active valves. The analysis is done by means of blood flow simulation into the pump and the prediction of platelets activation. The last is a measure of the pump compatibility with human life.**

The platelet activation state is evaluated by an equivalent or representative shear stress and compared with bibliographic data corresponding to other VAD kinds and cardiac prosthetic valves. The results show that, for the complementary blood flow rate supplied by the simulated VAD, the predicted platelet damage is in the same levels of current cardiac devices, particularly other VADs.

Keywords— **Ventricular assist device, blood damage, platelet activation, pulsatile flow.**

I. INTRODUCTION

Ventricular assist devices (VADs) are pumps that work in parallel with heart, pumping blood from the left ventricle to the aorta. They are used as a temporary solution for patients awaiting heart transplant, or as final therapy when heart replacement is not possible. The VAD's function is to restore the phisiologic flow helping the insufficient heart. Implantable VADs allow long term care with life quality improvement for patients, allowing them to do some normal activities.

Blood damage (BD) is one of the most significant aspects for the design and operation of VADs, the BD is

rate at which they are applied are the causes of platelet activation (PA) and hemolysis (H). These phenomena can trigger the coagulation cascade and produce a thrombogenic event that, in some cases, can produce death. Thus, it is necessary to limit PA and H, for wich VADs always require in vitro tests before in vivo use. Due to the cost of tests, computer simulations are a useful predictive tool before them.

The undesired effects of PA and H are also caused by prosthetic mechanical heart valves (MHV) and other devices. In this sense, two idexes are used to evaluate the performance of the VADs: the normalized index of hemolysis called NIH, which is standardized by the American Society for Testing and Materials (ASTM); and the rate of platelet activation called PAS, based on chemically modified prothrombinase test, proposed by Jesty and Bluestein (1999).

Hemolysis and platelet activation are complex processes because they depend on physical, chemical and physiological factors, but the shear stress is the main cause from the mechanical standpoint. Alemu and Bluestein (2007) described that while the RBCs resist 150 to 250 Pa for 100 seconds, the PLs resist 10 to 30 Pa in the same period of time. Since a decade ago computer simulations of blood flow into devices are used to predict the level of NIH and PAS based on the shear stresses (Alemu and Bluestein, 2007; Nobili *et al.*, 2008).

In this work, PA of blood flowing into a VAD, designed as a pulsatile pump based on a double effect piston, was analysed. For this purpose and due to the high computational cost, blood flow was simulated in a simplified 2D configuration. As shown in a previous work (Di Paolo *et al.,* 2014), this preliminary VAD geometry has many advantageous flow features, such as relative low velocities and very short-time vortices, that could preserve blood from both hemolisis and thrombosis. This asumption is reinforced here, because the results from cumulative damage model on platelets show that the device would produce flow conditions of low intensity interaction with blood, allowing long term use.

II. METHODS

A. VAD's description

The simulated VAD is a double effect volumetric pump. It consists of a cylinder which is driven via (not shown here), a left (LC) and a right (RC) chamber, two inlet (IV) and two output (OV) active valves as depicted in Fig. 1. The piston moves in one direction (x) with sinusoidal displacements and each piston stroke is used to pump fluid in one chamber and fills the other in alternating way. Between the chamber walls and the piston there is a small gap of 100 μm, which is supposed constant, i.e. the piston is mantained in y position by a magnetic field without contact. At the same time, this magnetic field is supposed to be the driven force to move the piston along x axis. The opening and closing of the valves is
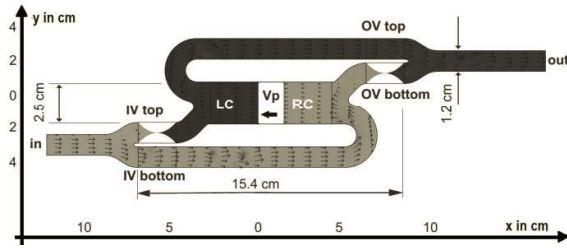
Figure 1. Simplified VAD's geometry. It is showing the input (in) and output (out) regions with piston moving from the right to the left and some global dimensions. LC: left chamber, RC: right chamber, IV: inlet active valve, OV: output active valve.

prescribed, in order to act syncronously with the piston displacement and the associated filling and emtying of the chambers. This means that the motion of the valves is electro-mechanically controlled.. Additionally, this mechanism allows to close a valve and to open its antagonistic with a delay (for example IV top and OV top of the LC) respect to the time in wich the piston begins to pump blood. This delay ensures that the valves in the same chambers are never open at the same time.

B. Flow model
A 2D geometry (see Fig. 1 and 2) is considered as a simplification of the 3D case, assuming blood as an incompressible and Newtonian fluid as it was discused in Fraser *et al.* (2010) and Behbahani *et al.* (2009). The flow is modeled by the continuity and Navier-Stokes equations and then, the set of equations are solved by means of finite elements method (FEM). Also, an appropriate coordinate mapping is used to trace the boundary displacement and mesh deformation, as described in the next section.

1) Moving domain and mesh deformation:
Equations (1) and (2) govern the harmonic motion imposed to the piston, xp and vp are the positon and velocity respectively, where $A = 2.0$ cm is the half piston stroke and $f = 2.1$ Hz is the frequency. An Arbitrary Langrangian-Eulerian formulation (ALE) and a deformable mesh technique as it was described by Donea *et al.* (2004), are implemented to manage the flow domain deformation during the piston motion. In addition, the valves opening and closing are simulated by imposing displacements to their respective boundaries but, to prevent the mesh collapse when valves close, a prescribed minimum gap was setted. The method is based in a previous work (Di Paolo *et al.*, 2014) but here a phase shift (delay) between the valve motions is introduced to avoid that the two valves remain simultaneously open in the same chamber. The valves opening/closing time is set at 26 ms.

2) Boundary conditions:
On fixed and moving solid surfaces, no-slip and impermeability boundary conditions are considered. Thus, $v = 0$ on the chamber and duct walls, $v = vp$ on the piston wall and $v = Vv$ on the valve boundaries. The time derivative of the position valve Dv presented in Eq. (3) is Vv, defined in Eq. (4). On the input and output sections, reference pressures are imposed: $Pin = 0$ and

$Pout = 13.3$ kPa (~ 100 mmHg), being this difference an approach of the mean aortic pressure drop. Furthermore, constant values are assumed for the viscosity and blood density: 1.060×10^3 kg/m^3 and 3.5×10^{-3} Pa s, respectively.

The deformation of the cross section due to the opening and closing of the valves is modelled by the function Dv that describes the valve behavior. Then, there are four equations having a general form given by Eq. (3). This function describes the displacement of each node, relative to the valve's centroid (X_0, Y_0), i.e. the centroid of the rectangles labelled Dv in Fig. 2.

$$xp = A\sin(2\pi ft) \tag{1}$$

$$vp = 2\pi fA\cos(2\pi ft) \tag{2}$$

$$Dv = \hat{a}\hat{b}St_n(t) \tag{3}$$

$$Vv = \hat{a}\hat{b}\frac{dSt_n(t)}{dt}\frac{dTT_n(t)}{dt} \tag{4}$$

$$\hat{a} = 1 - \left[\frac{(X - X_0)}{X_M}\right]^2 \tag{5}$$

$$\hat{b} = R_{ef}(Y - Y_0) \tag{6}$$

$$St_1(t) = \frac{-1}{1 + e^{-k(TT_1(t)-1)}} \tag{7}$$

$$St_2(t) = \frac{-1}{1 + e^{-k(TT_2(t)-1)}} \tag{8}$$

$$TT_1(t) = \cos(2\pi f(t + T) + CT) \tag{9}$$

$$TT_2(t) = \cos(2\pi f(t - 0.5T) + CT) \tag{10}$$

where $\hat{a}$ is a dimensionless parameter (Equation 5 governs the parabolic distribution of nodes on the X axis while X_M is the rectangle width), $\hat{b}$ is a length parameter (Equation 6 governs the linear distribution of nodes on Y axis and R_{ef} is the percentage of maximum valves closing (0.98%)) and $St_n(t)$ are dimensionless parameters that represent the valves temporal behavior (They depend on time, varying between 0 and -1).

While two valves work with the same temporal behavior ($St_1(t)$), the other two valve work in the same way but with a temporal delay ($St_2(t)$), therefore only two Eqs. (7) and (8) are defined, where k allows to adjust the valve opening and closing speed. Equations (9) and (10) define $TT_1(t)$ and $TT_2(t)$, they are cosinusoidal functions to establish the valve working cycle depending on the dimensionless constant CT. In this work, $k = 20$ was adopted to fix the opening and closing time in about 26 ms, and $CT = 1.20$ was selected to assure the
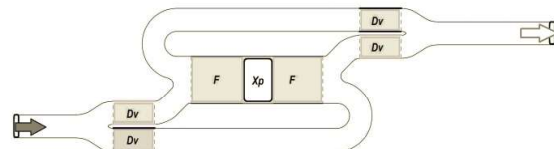

Figure 2. FEM mesh in different regions of the domain: mesh without deformation (in white), deformable mesh (in grey). Mesh regions in the chambers (F) are deformed according to the movement of the piston (vp) and mesh regions in the valves are deformed accordingly their movements (Vv). The input and output sections are indicated with dark grey and white arrows respectively.

opening of a valve when its antagonist is already closed (both in the same chamber).

The 2D geometry is discretized by a mesh of approximately 220,000 triangular elements of P3-P2 type, with sizes between 2×10^{-4} m and 5×10^{-3}m. These values show to be suitable according to the performed mesh refinement tests. These values are suitable according to mesh refinement tests. The simulation interval is of 1.0 s that corresponds to 2.1 cycles of piston motion (starting from the centre to the right) with maximum time-steps of 5×10^{-4} s.

A standard Galerkin mixed formulation is used with SUPG stabilization. Also, to start the simulation a high viscosity is used which quickly reach its desired value, while flow velocities and pressure are initialized with zero. Therefore, the results for the first half cycle are not considered for the analysis.The model was solved with the software COMSOL Multiphysics 3.5 running on a PC with an Intel Core i5 2500K 3.3 GHz processor and 16 GB of RAM. A fully -implicit, fully coupled Newton's method is choosen to linearize the equations and a direct solver (PARDISO) is used to solve the equation system in each iteration. The total simulation time is about 96 hours.

C. Model of blood damage

Modeling platelet activation phenomenon is complex. If it considers only physical aspects, platelet activation state (PAS) could be predicted using a model based on the rate at which the shear stress is applied. This model should consider, also, the history of shear stress acting on the cells. Thus, in this work the model proposed by Nobili et al. (2008) was adopted. For its application, the path of a set of PLs drifting in the flow domain must be known. For that purpose, it is supposed that the PLs moves massless-like virtual particles and their path are computed by integration of the velocity field. Then, the equivalent shear stress (τ) is evaluated for each PL (particle) path by Eq. (11) proposed by De Tulio et al. (2009). Finally, the shear stress history is used in Eq. (12) to evaluate the PAS_n, that is the PAS for the n-PL, where the constants a, b and C were extracted from Nobili et al. (2008). A global quantity $PASmean$ can be computed as the average of all PAS_n by means of Eq. (13), over a set of PLs released at the same time in a given region. In this work, three groups, each one composed for two sets of $N = 20$ and $N = 50$ particles representing the PLs, were released.

$$\tau = \frac{1}{2}\sqrt{\left(2\mu\frac{\partial u}{\partial x} - 2\mu\frac{\partial v}{\partial y}\right)^2 + 4\left[\mu\left(\frac{\partial u}{\partial y} + \frac{\partial v}{\partial x}\right)\right]^2} \quad (11)$$

$$PAS_n = \sum_{i=1}^{N} Ca\left[\sum_{j=1}^{i}\left(\tau(t_j)^{b/a}\Delta t_j + D_o\right)\right]^{a-1}\tau(t_i)^{b/a}\Delta t_i \quad (12)$$

$$PAS_{mean} = \frac{1}{N}\sum_{n=1}^{N} PAS_n \quad (13)$$

The model used to evaluate the $PASmean$ is, the most used by the community of reserchers and the most cited in literature (Bluestein et al., 2002; Alemu and Bluestein, 2007; Nobili et al., 2008; Sheriff et al., 2013). It predicts the platelet activation because of shear stress from physiological or artificial source. This cumulative damage model was adapted to represent experimental situations of pulsating shear stress, in this case the model works appropriately as described by Nobili et al. (2008). However, there are situations in wich the model can not properly represent the sensitization of PL under high shear stress and facilitating the subsequent platelet activation as described by Sheriff et al. (2013).

It is important to note that numerical simulation of platelet activation is an open study field and there is not an optimal model for all situations of blood flow (natural or artificial). The model used in this study was modified by Sheriff et al. (2013), incorporating new parameters to better represent blood damage in many flow situations. However, these researchers have pointed out model limitations to represent certain in vitro results due to the power law description (see Eq. 12).

D. Platelet path

The platelet path strongly depends on the initial conditions. These should correspond to position and time where no overflow or backflow happen. For that reason, initial positions after the bifurcations were selected. The instants of 150 ms and 390 ms were selected to avoid the use of the first semicycle of the simulation, being these the times when flow begins to accelerate into the RC and LC respectively.

The initial positions of N platelets are assumed to be distributed along a line where coordinate x is constant. In this paper, the path of three (3) groups of platelets were analized.The groups are listed below:

Group 1: Corresponds to PLs released at time 150 ms, moving from the IV top. This group passes through the LC and is composed by two series: Serie 1 with $N = 20$ and serie 2 with $N = 50$.

Group 2: Corresponds to PLs released at time 150 ms moving from the IV bottom. This group passes through the RC and is composed by two series: Serie 3 with $N = 20$ and serie 4 with $N = 50$.

Group 3: Corresponds to PLs released at time 390 ms from the center of the RC and passing through the OV bottom, it is composed by two series: Serie 5 with $N = 20$ and serie 6 with $N = 50$.

III. RESULTS

A. Blood flow into the VAD

The outflow rate can be seen in Fig. 3, it is the addition of three different contributions: a) the flow that drives the piston, whose shape is a "rectified sine", b) the flow due to the closing of OV (positive peak) and c) the reflux because of the opening of the other OV (negative peak).

This flow rate behaviour is because in the simulation, the movement of a valve sweeps an area not negligible compared to the area that sweeps the piston. So, the outflow reaches a maximum flow rate of 120 cm²/s, while the backflow reaches a minimum of -100

cm^2/s (see Fig. 3). Also, it can be seen in Fig. 3 the effect of the delay between the closing and opening of the two OV, that is the same delay that acts between the antagonist valves in each chamber. The mean outflow rate is about 39.3 cm^2/s; considering a 2.0 cm width, the pump could provide a flow rate of 78 cm^3/s, that is 4.7 l/min, which is enough flow rate to complement an insufficient heart. A similar situation happens with the inlet flow rate, but in this case the negative peak appears first and then appears the positive peak.

Figure 4 shows zooms of flow velocity at input and output regions, at the instants when piston has its maximum velocity going from left to the right and starts a new stroke. The situation ploted in Fig. 4-a shows that the maximum fluid velocity appears in the gap of IV bottom, because of the backflow coming from the pumping chamber (RC), and Fig. 4-b shows the maximum flow velocity at the gap of OV top, when the new piston stroke starts to pump from LC and this valve starts its opening. At this time, a backflow is flowing from the output to the LC. Both situation indicates that velocities are highest at the valve gaps.

B. Pressure in VAD chambers

When VAD operates, pressure in the pumping chamber is greater than the external pressure (*Pout*) to allow the exit of flow rate while in the other chamber, a lower pressure (negative) is generated to allow the entry of blood for the next stroke. In Fig. 5 it can be seen the pressure variation with time in the LC: during a half period it acts as a driver chamber while RC acts as a suction chamber. The pressure generated by the piston movement and the opening/closing of the valves reach a maximum value of 25 kPa and a minimum value of about -12 kPa.

Similarly, the same sequence of events happens for pressure variation in the RC, but with a difference of a half cycle. Moreover, conditions of the pressure field can be seen in Fig. 1 where the grey (*Pin*) and black (*Pout*) represent the pressure in each chamber and ducts. When the piston is in the position corresponding to half stroke ($xp = 0$), the pressure in each chamber are instantaneously equilibrated with values imposed at input or output respectively (see in Fig. 5 the points where pressure in LC has 0 value and 13.3 kPa).

C. Shear Stress

The maximum equivalent shear stress value can be seen in Fig. 6 for the times: 476 ms (a) and 595 ms (b). There is a relationship between the locations of high speed vortices and the sites where τ is high. Although τ does not exceed 4.0 Pa at the inletflow region, there are certain areas where the maximum shear stress (τ_max) is highest for a very short instant. Areas of high shear streses can be seen in Fig. 6 (black color areas) which are: a) the pipe joints (or vifurcations) of the input and output branches, during the opening and closing of the valves (up to 155 Pa); b) the vortices that appear near the valves at the instants of opening or closing; c) the apex of valves, where τ reaches a maximum of 80 Pa at
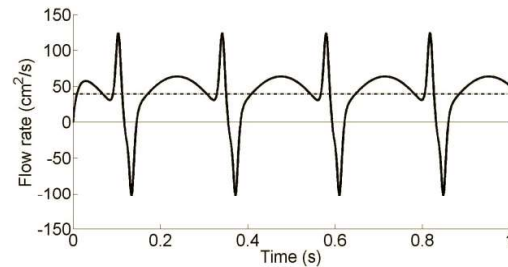

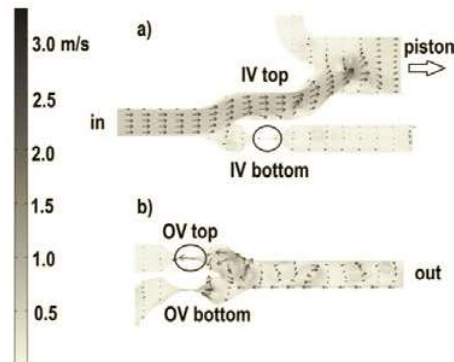Figure 3. Outflow rate. The mean flow rate is indicated with dashed line.

Figure 4. Velocity field: a) zoom of the input at 476 ms, with maximum $vp = 0.27$ m/s; the black circle indicates the region where is the maximum fluid speed (1.71 m/s); b) zoom of the output at 595 ms, with vp=-0.01 m/s; the black circle indicates the region where is the maximum fluid speed (3.28 m/s).
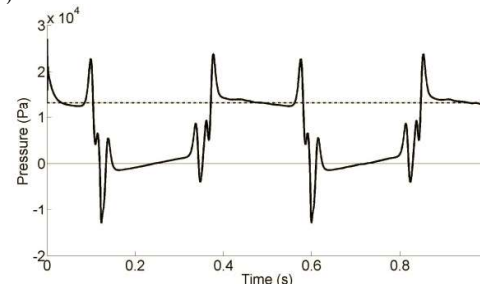

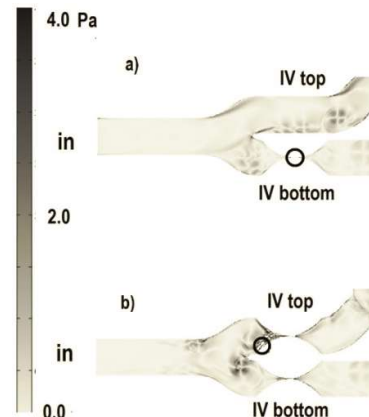Figure 5. Pressure into LC versus time evaluated at a corner of the piston. The *Pout* is indicated with dashed line.

Figure 6. Representative shear stress at the input. In each figure the black circle indicates the maximum: a) τ_{max}= 56 Pa at $t = 476$ ms and b) $\tau_{max} = 65$ Pa at $t = 595$ ms.
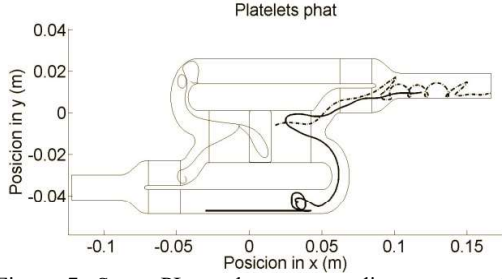
Figure 7. Some PLs paths corresponding to examples of: group 1 (gray thin line), group 2 (black thick line) and group 3 (thick dashed line). The y dimension has been shifted to better comprehention.
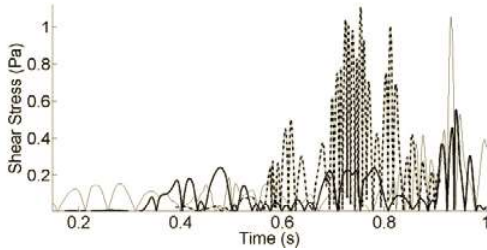

Figure 8. Equivalent shear stress for each path sowed in the Fig. 7: group 1 (thin gray line), group 2 (thick black line) and group 3 (thick dashed line).

the closing instant and d) the DAV elbows where τ is below than 20 Pa when outflow rate is maximum.

Typical paths for each group can be observed in Fig. 7; whereas Fig. 8 shows the equivalent shear stress acting on each PL of Fig 7. Also, Fig. 9 depicts the PAS_n for each PL of Fig. 7, obtained by Eq. (12).

For the first two groups (series 1, 2, 3 and 4) between 150 and 1000 ms it was observed that all PL do not leave the DAV. In turn, in the third group (series 5 and 6), whose travel is computed in the period between 390 and 1000 ms, some PL quickly travel into RC crossing the output section and exiting VAD as seen in Fig 8. When a platelet start near walls, its low movement can possibilitate that PL remain into a vortex for a long period of time, as can be seen in a trajectory of Fig. 7.

D. Platelet activation

Figure 8 show that the τ on each path analyzed does not exceed 1.0 Pa. In relation to Eq. (12), which takes into account the memory of PL and the gradient of the shear stress acting on them, the maximum values of PAS_n for each generated path do not exceed 2.0×10^{-6} and, in most cases, the final value is between 1.0×10^{-6} and 2.0×10^{-6}.

Figure 10 shows the mean growing slope of the $PASmean$, nothing that all curves have the same average value of 2.85×10^{-6} 1/s ($2.0 \times 10^{-6}/0,700$ s). Also, It is noted that $PASmean$ obtained for other sets of paths in the same time interval (150 ms to 1000 ms), do not exceed the value of 2.0×10^{-6} with the same mean slope to $PASmean$ showed in Fig. 10.

IV. DISCUSSION

The maximum τ value (Fig. 8) is much lower than the yield strength of platelets. In this sense, an approximated index of platelet activation may be obtained as the product of shear stress by the elapsed time. The results of this work predict a value of 1.0 Pa s for the index of platelet activation. This value is lower than the Hellums *et al.* (1987) limit criterion (3.5 Pa s), being a tolerable platelet activation value.

The predicted *PASmean* results reach similar levels of those reported by Morbiducci *et al.* (2009), 1.80×10^{-6} for the analysis of a MHV over a period of simulation of 350 ms. On the other hand, the value of *PASmean* obtained in this work for a period of circulation of 850 ms, is around 2.00×10^{-6} and is expected to continue growing with a mean rate of 2.85×10^{-6} 1/s. Also, the *PASmean* level for different groups of PL, depends directly on overall time in which shear stresses are applied.

Platelets have a mean life of 10 days and, in this period, can pass hundreds to thousands times through heart. In the case of a person with an implanted VAD it is more probable that a PL pass through it, because the heart, pumps a small fraction of the total flow rate. Considering the maximum measured *PASmean* level of 2.0×10^{-6}, if each PL passes 1,000 times and assuming a cumulative damage into the VAD, then a value of 0.002% of the normalized PAS would be reached in every step. Such low prediction of blood damage, encourages us to develop advanced studies on the simulated device.

Furthermore, taking into account the growing gradient of *PASmean* of 2.85×10^{-6} 1/s, it would be required 65 minutes to reach 0.01% of *PASmean*. The *PASmean* for this VAD is lower in comparison with value obtained in the test developed by Bluestein *et al.* (2010). While the Bluestein VAD reached a level of 0.01% in 30 min, for the same level, the device presented in this paper would take approximately 65
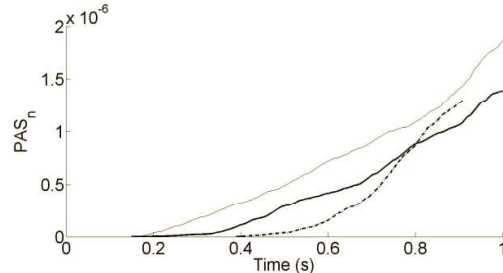

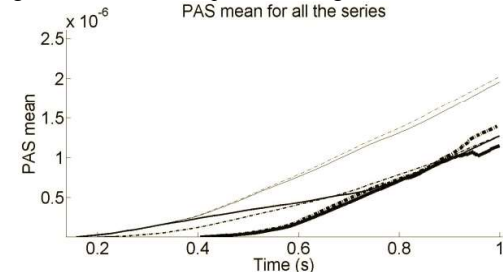Figure 9. PAS_n for each path of the Fig. 7.

Figure 10. PAS*mean* for all series: serie 1 (gray thin line), serie 2 (gray thin dashed line), serie 3 (black line), serie 4 (black dashed line), serie 5 (black thick dashed line), serie 6 (black thick line).

min. This is a promising situation for the concept of VAD proposed in this work.

V. CONCLUSIONS

A proposed new model of a pulsatile ventricular assist device with a double effect piston and four valves, was numerically analized in this work. This preliminary VAD geometry has many advantageous charateristics for blood flow related to low risk of hemolisis and thrombosis. Also, results oriented to evaluate some crucial variables for testing the biological and mechanical performance of the VAD were obtained. However, in future simulations the valve´s motion is a topic that merits more analysis.

The platelet activation produced by flow, is comparable to current pulsatile VADs and MHV. Nevertheless, predictions obtained must be corroborated by further research because the important objective to achieve a suitable VAD.

The information obtained from the two-dimensional model serves as a starting point for future simulation. Therefore, a 3D analysis in a more realistic geometry is needed for which very high computational costs are expected. Also, it is possible reduce the computational cost of 3D simulation by means of an appropriate turbulent flow model.

REFERENCES

Alemu, Y. and D. Bluestein, "Flow-induced Platelet Activation and Damage Accumulation in a Mechanical Heart Valve: Numerical Studies," *Artificial Organs*, **31,** 677–688 (2007).

Behbahani M., M. Behr, M. Hormes, U. Steinseifer, D. Arora, O. Coronado and M. Pasquali, "A Survey in Mathematics for Industry. A review of computational fluid dynamics analysis of blood pumps," *Euro. Journal of Applied Mathematics*, **20,** 363–397 (2009).

Bluestein D., B. Chandran y K. Manning K., "Towards Non-thrombogenic Performance of Blood Recirculating Devices," *Ann. Biomed. Eng.*, **38**, 1236–1256 (2010).

Bluestein, D., Y. Li and I. Krukenkamp, "Free emboli formation in the wake of bi-leaflet mechanical heart valves and the effects of implantation tecniques," *Journal of Biomechanics*, **35**, 1533–1540 (2002).

De Tullio D., A. Cristallo, E. Balaras and R. Verzicco, "Direct numerical simulation of the pulsatile flow through an aortic bileaflet mechanical heart valve," *J. Fluid Mech.*, **622,** 259–290 (2009).

Di Paolo J., J.F. Insfrán, E. Fríes, D.M. Campana, M.E. Berli and S. Ubal, "A preliminary simulation for the development of an implantable pulsatile blood pump," *Advances in biomechanics and applications,* **1,** 127-141 (2014).

Donea J., A. Huerta, J. Ponthot and R. Ferran, "Arbitrary Lagrangian-Eulerian Methods," *Encyclopedia of Computational Mechanics*, E. Stein, R. de Borst and T.J.R. Hughes (Eds.), *John Wiley & Sons, Ltd.* (2004).

Fraser, K.H., M.E. Taskin, B.P. Griffith and Z.J.Wu, "The use of computational fluid dynamics in the development of ventricular assist devices," *Medical Engineering & Physics,* **33**, 263–280 (2010).

Jesty J. and D. Bluestein, "Acetylated prothrombin as a substrate in the measurement of the procoagulant activity of platelets: Elimination of the feedback activation of platelets by thrombin," *Anal Biochem*, **272**, 64–70 (1999).

Hellums, J., D. Peterson, N. Stathopoulos, J. Moake and T. Giorgio, "Studies on the Mechanisms of Shear-Induced Platelet Activation," *Cerebral Ischemia and Hemorheology,* A. Hartmann and W. Kuschinsky (Eds.), Springer-Verlag, Berlin, 80-89 (1987).

Nobili, M., J. Sheriff, U. Morbiducci, A. Dedaelli and D. Bluestein, "Platelet Activation Due to Hemodynamic Shear Stresses: Damage Accumulation Model and Comparison to In Vitro Measurements," *ASAIO J*, **54,** 64–72 (2008).

Morbiducci, U., R. Ponzini, M. Nobili, D. Massai, F. Montevecchi, D. Bluestein and A. Redaelli, "Blood damage safety of prosthetic heart valves. Shear-induced platelet activation and local flow dynamics: A fluid–structure interaction approach," *Journal of Biomechanics,* **42**, 1952–1960 (2009).

Sheriff, J., J.S. Silva Soares, M. Xenos, J. Jesty and D. Bluestein, "Evaluation of Shear-Induced Platelet Activation Models Under Constant and Dynamic Shear Stress Loading Conditions Relevant to Devices," *Ann. Biomed. Eng.*, **41,** 1279–1296 (2013).